ANTENNA STRUCTURE AND EXCITATION DYNAMICS IN PHOTOSYSTEM I

I. Studies of Detergent-isolated Photosystem I Preparations Using Time-resolved Fluorescence Analysis

T. G. OWENS,* S. P. WEBB,‡ R. S. ALBERTE,* L. METS,* AND G. R. FLEMING‡
*Department of Molecular Genetics and Cell Biology and ‡Department of Chemistry, University of Chicago, Chicago, Illinois 60637

ABSTRACT The temporal and spectral properties of fluorescence decay in isolated photosystem I (PS I) preparations from algae and higher plants were measured using time-correlated single photon counting. Excitations in the PS I core antenna decay with lifetimes of 15–40 ps and 5–6 ns. The fast decay results from efficient photochemical quenching by P700, whereas the slow decay is attributed to core antenna complexes lacking a trap. Samples containing core and peripheral antenna complexes exhibited an additional intermediate lifetime (150–350 ps) decay. The PS I core antenna is composed of several spectral forms of chlorophyll *a* that are not temporally resolved in the decays. Analysis of the temporal and spectral properties of the decays provides a description of the composition, structure, and dynamics of energy transfer and trapping reactions in PS I. The core antenna size dependence of the spectral properties and the contributions of the spectral forms to the time-resolved decays show that energy is not concentrated in the longest wavelength absorbing pigments but is nearly homogenized among the spectral forms. These data suggest that the "funnel" description of antenna structure and energy transfer (Seely, G. R. 1973. *J. Theor. Biol.* 40:189–199) may not be applicable to the PS I core antenna.

INTRODUCTION

The utilization of incident light energy by photosynthetic organisms involves the absorption of light by a variety of light-harvesting antenna pigments and the subsequent transfer of excited state energy to the photochemical reaction centers. Light-harvesting and reaction center pigments are specifically bound in a variety of pigment-protein complexes whose composition, structure, and function have been characterized by a number of biochemical and biophysical techniques (for review, see reference 1). Energy transfer from antenna to reaction center pigments occurs in the form of mobile excited states (excitations) that migrate between pigments by an incoherent Förster mechanism (2, 3). The efficiency and directionality of excitation transfer reactions depends upon the relative position, orientation, and spectral properties of pigments within the pigment-protein complexes and between interacting complexes in the photosynthetic apparatus.

A detailed understanding of the structural and functional relationships between antenna and reaction center complexes is a prerequisite to describing the processes that regulate excitation transfer and photochemical trapping reactions. The analysis of fluorescence decay kinetics using time-correlated single photon counting is recognized as a valuable tool for studying excitation transfer reactions and the structural organization of photosynthetic light-harvesting systems (4, 5). Using low-intensity picosecond excitation lasers and fast microchannel plate detectors, the technique has the potential for resolving complex multiexponential decays (6) with time resolution better than 10 ps (7, 8). The ability to resolve multicomponent decays is critically important considering the complexity of the photosynthetic apparatus. Oxygen-evolving organisms contain two types of reaction centers which are in turn associated with several distinct types of antenna complexes. The various spectral forms of light-harvesting pigments associated with each photosystem may potentially contribute unique decay components to the overall fluorescence decay profile. The assignment of these fluorescence decay components to functional pigment aggregates within the photosynthetic apparatus is essential to structural analyses and to a description of excitation migration and trapping reactions. The contribution of pigment interactions within and between pigment-binding subunits of C-phycocyanin

Address correspondence to Thomas G. Owens, Section of Plant Biology, Plant Science Building, Cornell University, Ithaca, NY 14853-5908.

Address reprint requests to G. R. Fleming, Department of Chemistry, University of Chicago, 5735 S. Ellis Ave., Chicago, IL 60637.

(7, 9) demonstrates the potential complexities of in vivo fluorescence decay within a single type of light-harvesting aggregate.

Measurements of room temperature fluorescence decay in isolated chloroplasts or intact algal cells indicates that a minimum of four exponential components are required to accurately describe in vivo fluorescence decay (10–12). In each case, three of the decay components were assigned to pigment aggregates associated with PS II. The fourth component was attributed to excitation decay in PS I and exhibited lifetimes between 30 and 90 ps, amplitudes of 0.1 to 0.55, and a lack of sensitivity to PS II redox state. In agreement with room temperature steady-state measurements (13), emission of the PS I decay component was red-shifted (emission maximum at ≈700 nm) compared with PS II pigments and had a very low fluorescence yield ($\approx 10^{-3}$). Recent measurements with isolated PS I preparations demonstrated that the short lifetime of excitations in PS I is limited by efficient photochemical quenching on P700 (8).

The antenna complexes associated with PS I can be broadly divided into two categories: the core and peripheral antenna complexes (14). The PS I reaction center/core antenna complex has been isolated using a number of techniques (14–17); the polypeptide and pigment composition, spectral properties and core antenna size (chl *a*/P700 ratio) of these preparations vary slightly depending on the isolation procedure. The core antenna consists of several spectral forms of chl *a* (15), that along with the P700 reaction center are bound exclusively to two similar polypeptides in the 60–70 kD range (16, 18). These polypeptides also bind the initial PS I acceptors A_0, A_1, and F_x ($=A_2$) (19). Five additional polypeptides in the 8–20 kD range may also be found in the PS I reaction center/core antenna preparations (20) and serve as structural components or as part of the PS I acceptor complex (19, 21). The peripheral antenna complexes of PS I contain both chl *a* and chl *b* bound to several related polypeptides in the 19–25 kD range (14, 22–25).

In a preliminary report of fluorescence decay kinetics in detergent-isolated PS I preparations and in mutants of the green alga *Chlamydomonas reinhardii* that lack the PS II reaction center, we observed that the number of exponential components required to accurately describe the decay profiles was dependent on the type of antenna complexes present in the sample (26). In samples containing only reaction center and core antenna pigments the fluorescence decay was clearly biphasic, whereas in samples containing both core and peripheral antenna pigments the decays were fit to three or more exponentials. In both types of samples, the major decay component (lifetime = 15–40 ps, amplitude 0.5 to 0.95) was attributed to excitations in the PS I core antenna. The lifetime of these excitations is linearly related to the PS I core antenna size (8, 26).

In the present investigation, we describe in detail the temporal and spectral properties of room temperature fluorescence decay in PS I preparations isolated in the presence of Triton X-100. The samples were derived from several plant and algal sources and contained varying amounts of core and peripheral antenna pigments. By analysis of the biochemical and biophysical properties of these samples, we present a structural and mechanistic description of excitation migration and trapping in PS I. A similar analysis of fluorescence decay in mutant strains of *C. reinhardii* lacking the PS II reaction center/core antenna complex will be detailed elsewhere (in preparation).

MATERIALS AND METHODS

Washed thylakoids were prepared from 12–17-d-old barley seedlings (*Hordium vulgare*, cv., Himalaya) using the procedure of Shiozawa et al. (15). *Chlamydomonas reinhardii* (wild-type strain DS-521) was grown in Tris-acetate-phosphate medium as described by Surzycki (27). *Synechococcus sp.* (clone SYN) was grown in natural seawater medium enriched with f/2 nutrients (28). Algal cells were harvested by centrifugation and resuspended in 100 mM Tris-Cl, 100 mM NaCl, 2 mM $MgCl_2$, 1 mM EDTA (pH 8.0) at 1.5 mg chl *a* + *b*/ml. Cells were disrupted by two passes through a French Pressure Cell at 6,000 psi. Whole cells and cell wall debris was removed by centrifugation at 8,000 *g* for 5 min. Broken thylakoids were collected by centrifugation at 32,000 *g* for 10 min and were washed three times in 50 mM Tris Cl, 0.1 mM EDTA (pH 8.0).

The P700 Chl *a*–protein complex was isolated from washed thylakoids using the procedure of Shiozawa et al. (15) as modified by Owens et al. (8). Thylakoids were solubilized in 1% Triton X-100, 50 mM Tris-Cl, pH 8.0, at Triton:chl *a* + *b* ratios between 60 and 100. Treatments were for 10–30 min at 4°C in the dark. Insoluble material was removed by centrifugation at 36,000 *g* for 10 min. The pigmented extract (5–10 mg chl *a* + *b*) was loaded on a hydroxylapatite column (25 ml packed vol) that was preequilibrated with 10 mM Na phosphate, pH 7.0. After washing the column with one volume 10 mM Na phosphate, pH 7.0, and four volumes 50 mM Tris-Cl, pH 8.0, containing 1% Triton X-100, the pigmented hydroxylapatite was removed from the column and made into a slurry with 25 ml 1% Triton X-100, 50 mM Tris-Cl, pH 8.0. After stirring the suspension continuously for 10 min at 4°C in the dark, a 0.5-ml aliquot was removed for pigment analysis. The hydroxylapatite was then pelleted and the 1% Triton X-100 wash procedure was repeated until the preparation contained no detectable chl *b* and the chl *a*:P700 ratio no longer declined. Pigment was released from sedimented hydroxylapatite by briefly washing in 10 mM Na phosphate, pH 7.0, followed by elution in 0.2 M Na phosphate, pH 7.0, containing 0.05% Triton X-100.

Photosystem I complexes containing chl *b* were prepared by reducing the Triton concentration in the initial solubilization step (Triton/chl = 40–60) and by reducing the number of detergent washes of the hydroxylapatite-pigment slurry. In samples containing significant amounts of chl *b*, detergent-solubilized pigments and isolated light-harvesting complexes that coeluted from the hydroxylapatite were separated from functionally coupled PS I aggregates by centrifugation on a sucrose density gradient (14).

Chlorophylls *a* and *b* were determined spectrophotometrically in 90% acetone extracts (29). P700 was measured in 0.05% Triton X-100 extracts by light-induced absorbance changes at 697 rm (15) using a differential extinction coefficient of 64 $mM^{-1}\ cm^{-1}$ (30). Chlorophyll *a* content of the 0.05% Triton extract was estimated using an extinction coefficient of 60 $mM^{-1}\ cm^{-1}$ at 677 nm (31). Polypeptide composition of the preparations was determined by SDS-PAGE. Proteins were precipitated from the Triton extract in cold (−20°C) acetone. Absorption and fluorescence emission spectra were recorded using an Aminco DW-2 spectrophotometer and SPF-1000 spectrofluorometer, respectively. Emission spectra were corrected for variations in source intensity and detector sensitivity.

Fluorescence decay measurements were performed using time-correlated single photon counting as previously described (8, 11). Excitation was provided by a synchronously pumped DCM dye laser that was cavity dumped at 75.6 kHz. Pulses had a FWHM of 6–8 ps and a maximum intensity of 3×10^{11} photons cm^{-2} $pulse^{-1}$ at 655 nm. The excitation was attenuated such that all samples absorbed <0.05 photons per reaction center per pulse. Samples (OD = 0.6 at 672 nm) were placed in a temperature regulated cuvette at 10°C and were stirred continuously during analysis. Samples for low-temperature analysis were diluted 1:1 in glycerol. Fluorescence photons were collected at 90° to the excitation through a 0.75-mm slit. Fluorescence was selected by a grating monochromator (bandpass = 4 nm) and detected by a red-sensitive microchannel plate (Hamamatsu R1645-01μ) that was cooled to reduce dark counts.

The instrument response function was measured by scattering the excitation pulses with a dilute solution of nondairy creamer in water and had a FWHM of 60–80 ps and a full width at $1/10$ maximum of 130–150 ps. The true fluorescence decay function (response to a delta-function excitation, F[t]) was described as a weighted sum of simultaneous exponential decays:

$$F(t) = \Sigma A_i \exp(-t/\tau_i),$$

where

$$\Sigma A_i = 1.0,$$

and A_i and τ_i are the preexponential amplitudes and lifetimes, respectively, of each decay component, i. The measured fluorescence decay profiles were fit to $F(t)$ convoluted with the instrument response function using a nonlinear least squares program (32). The fitting routines contained a variable shift parameter, reflecting the time separation between the peaks of the fluorescence decay and instrument response functions (7), and were capable of detecting rising fluorescence associated with excitation transfer between pigment aggregates. Goodness of fit was judged by the reduced X^2 parameter and by the distribution of normalized residuals. Minimum time resolution of the system was ~8–10 ps. Unless otherwise noted, counting was terminated when 10^5 counts accumulated in the peak fluorescence channel. Variabilities in the measurement of the amplitude and lifetime of an individual decay component in replicate samples were <5 and 10%, respectively. Fluorescence excitation and emission spectra of the individual decay components were calculated by normalizing the preexponential amplitudes to a constant excitation intensity and constant measuring time (10, 33). This procedure makes no assumptions about the shape of the steady-state or time-resolved spectra. Emission spectra were also corrected for the wavelength-dependent response of the microchannel plate.

RESULTS

Composition of the P700 Chlorophyll *a*-Protein Complex

The antenna pigment composition of the PS I preparations isolated from barley seedlings and *C. reinhardii* by the modified hydroxylapatite wash procedure varied depending on the extent of 1% Triton X-100 washes and on the initial solubilization conditions. The preparations could be divided into two groups based on the enrichment of P700 in relation to antenna pigments and on the content of chl *b*. Preparations exhibiting chl *a*/P700 ratios <45 did not contain detectable chl *b* (chl $a/b > 300$ by high-pressure liquid chromatography analysis), whereas less enriched preparations (chl $a + b$/P700 = 63–115) had chl a/b ratios <20 (Table I). The polypeptide composition of all preparations showed a major band or pair of bands at 65–70 kD and several additional bands in the 15–25 kD range. In the more enriched preparations (24–43 chl *a*/P700), the content of the lower molecular weight polypeptides was noticeably reduced, especially the apoproteins of the peripheral antenna complexes that bind chl *a* and *b* (19–25 kD). The minimum chl *a*/P700 ratio of a preparation appeared to be determined during the initial solubilization step: increased Triton X-100/chl $a + b$ ratios and longer incubation times generally correlated with a greater enrichment of P700. Increasing the number of 1% Triton X-100 washes of the hydroxylapatite eventually lead to a rapid loss of photooxidizable P700, an increase in the chl *a*/P700 ratio and a decrease in the total pigment content of the final eluate.

The steady-state absorption spectra (10°C) of PS I preparations isolated from barley (chl *a*/P700 = 43), *C. reinhardii* (chl *a*/P700 = 41), and *Synechococcus sp.* (chl

TABLE I
SUMMARY OF TIME-RESOLVED FLUORESCENCE DECAY IN PS I PREPARATIONS

Source	chl/P700	chl *a/b*		i = 1	i = 2	i = 3	i = 4	X^2
Barley	24	>300	A_i	0.879	0.121			1.10
			τ_i	15.8	5971			
Barley	43	>300	A_i	0.917	0.083			1.07
			τ_i	25.9	6301			
Barley	78	18	A_i	0.592	0.198	0.113	0.097	1.52
			τ_i	24.8	253	2407	6174	
C. reinhardii	41	>300	A_i	0.856	0.144			1.13
			τ_i	25.5	5978			
Synechococcus sp.	55	—	A_i	0.883	0.117			1.14
			τ_i	29.1	5783			
Synechococcus sp.	122	—	A_i	0.541	0.134	0.178	0.147	1.37
			τ_i	37.7	258	784	5908	

All samples were isolated in the presence of Triton X-100. Decays were fit to the equation $F(t) = \Sigma A_i \exp(t/\tau_i)$. A_i, amplitude of decay component i; τ_i, lifetime (in ps) of decay component i; X^2, reduced chi-squared parameter.

a/P700 = 55) are compared in Fig. 1 *A*. Except for small differences in the chl *a* Soret and carotenoid (470–510 nm) absorptions, the spectra of all samples that lacked detectable chl *b* were very similar and characteristic of PS I reaction center/core antenna complexes isolated with nonionic detergents (15, 16). Preparations that contained chl *b* showed increased absorption at 470 and 650 nm (not shown).

The steady-state absorption (600–750 nm) and fluorescence emission (10°C) spectra from three different reaction center/core antenna preparations from barley with varying core antenna sizes (24, 33, and 43 chl a/P700) are compared in Fig. 1, *B* and *C*, respectively. All samples showed an absorption maximum at 677 nm and emission maxima at 682–683 nm. The normalized absorption spectra show only minor variability in the 650–670 nm region whereas the fluorescence emissions are equally similar. When samples were allowed to come to room temperature (22°C) for 30 min, an irreversible blue shift (≈5 nm) was observed in both the absorption and emission spectra. Mild heat treatment (30°C) also altered the time-resolved properties of the samples (see below).

Time-resolved Fluorescence Analysis

The fluorescence decay of a PS I reaction center/core antenna preparation from barley (chl a/P700 = 33) measured at 650 nm excitation and 690 nm emission is shown in Fig. 2. The decay is accurately fit (X^2 = 1.05) to the sum of two exponential decay components with 1/e lifetimes of 19.9 and 6,130 ps and amplitudes of 89.2 and 10.8%, respectively. Forcing the data to fit to three exponential components did not reduce the X^2 parameter or alter the distribution of normalized residuals, and generally resulted in two decay components with identical lifetimes. Reduction of the excitation intensity × 10 did not alter the fluorescence decay kinetics, indicating that excitation annihilation processes did not contribute to the observed decays. In addition, the decay kinetics were the same in stationary, stirred, or rapidly flowing samples suggesting that the accumulation of long-lived states did not affect the decay. The fluorescence decay kinetics of several PS I preparations from different sources are summarized in Table I. Samples which lacked chl *b* and had chl a/P700 ratios <55 exhibited a biphasic exponential decay, whereas samples less enriched in P700 (containing peripheral antenna pigments) displayed more complex decays. The occurrence of intermediate lifetime components (100 ps < τ < 5 ns) in PS I have been previously reported in detergent-free thylakoid fragments (34) and in mutants of *C. reinhardii* that lack the PS II reaction center complex (11, 26).

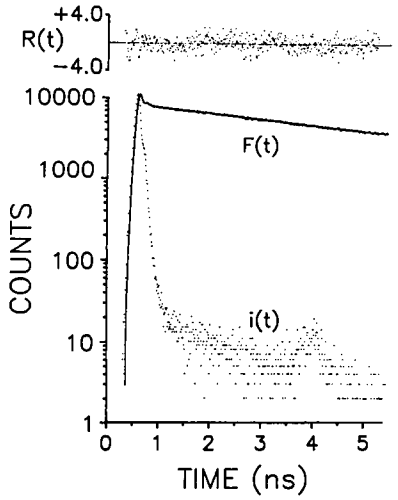

FIGURE 2 Fluorescence decay of a PS I reaction center/core antenna preparation from barley (chl a/P700 = 33). i(t), instrument response function. F(t) (*dots*), measured fluorescence decay profile. (*Solid line*), least squares fit of $F(t) = 0.892 \exp(-t/19.9\text{ ps}) + 0.108 \exp(-t/6{,}130\text{ ps})$ convoluted with i(t), X^2 = 1.05. R(t), normalized residuals from least squares regression. Excitation wavelength = 650 nm, emission collected at 690 ± 4 nm.

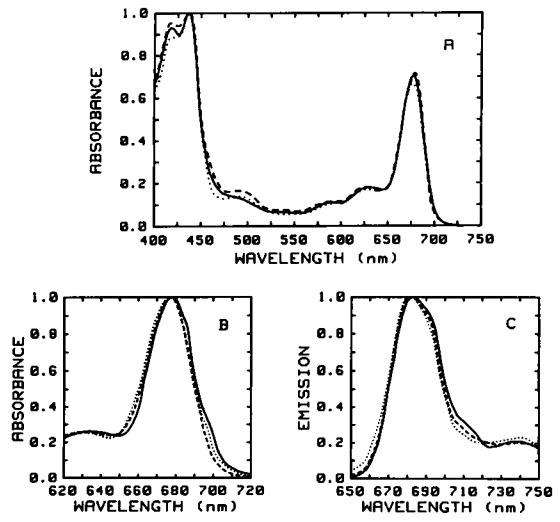

FIGURE 1 Steady-state absorption and fluorescence emission spectra of PS I preparations. (*A*) Visible absorption spectra of PS I preparations from barley (—), *C. reinhardii* (·····) and *Synechococcus sp.* (----). (*B*) Red absorption spectra. (*C*) fluorescence emission spectra of PS I preparations from barley with varying core antenna sizes. (·····) chl a/P700 = 24; (----) chl a/P700 = 33; (—) chl a/P700 = 43. All spectra recorded at 10°C.

The fluorescence decay in most samples was dominated by a fast 15–40 ps component, accounting for as much as 96% (an average of 89% in enriched samples lacking chl *b*) of the initial amplitude of the decay. The lifetime of excitations associated with the fast decay component has been shown to be limited by efficient photochemical quenching on P700 (8). Samples that lacked chl *b* also exhibited high photochemical quantum yields (>0.80). Samples that contained peripheral antenna pigments generally showed a reduced contribution of the fast component to the total decay. All samples examined in this study also exhibited a slow decay component (lifetime = 5.5–6.5 ns, amplitude = 5–20%) independent of the presence or absence of peripheral antenna pigments. Because the life-

time of the slow decay component approximates that of chl *a* in solution (5 ns) (35), it was initially assumed that this component should be attributed to a small amount of detergent-solubilized chl *a* in the preparation. Attempts to eliminate or reduce the amplitude of the slow component by further hydroxylapatite chromatography were unsuccessful.

Photosystem I reaction center preparations were also isolated from the marine cyanobacterium *Synechococcus sp.* These complexes had chl *a*/P700 ratios between 50 and 120 and contained no detectable PS II activity. The fluorescence decay properties of the *Synechococcus* preparations with chl *a*/P700 ratios <60 were nearly identical to the chl *b*–less preparations from barley (Table I). The longer lifetime of the fast decay component is again related to the larger core antenna size of the preparation (8). Preparations with chl *a*/P700 ratios between 65 and 130 exhibited more complex decays and additional decay components in the 250–850 ps range. These additional decay components accounted for as much as 50% of the initial amplitude of the decay in preparations with the largest antenna sizes (data not shown).

The stability of the PS I preparations, measured as the amplitude of the fast decay component remaining after 12 h at 5°C in the dark, is strongly affected by the concentration of Triton X-100 in the eluate. Fig. 3 shows the yield of P700 in the initial extract and the stability of the sample as a function of Triton concentration used to elute pigment from the hydroxylapatite. Although the yield is maximal at Triton concentrations between 0.05 and 0.7%, the stability of the preparation declines rapidly above 0.05% Triton.

The effects of exogenous electron donors and acceptors and of redox mediators on the fluorescence decay kinetics of a PS I preparation (chl *a*/P700 = 42) are summarized in Table II. Addition of small amounts of ascorbate and/or methyl viologen, which act as artificial donors and acceptors, respectively, had no affect on the decay kinetics. Addition of ferricyanide sufficient to completely oxidize all P700 (determined by light-induced photobleaching at 697 nm) also had no effect on the decay kinetics. Addition of

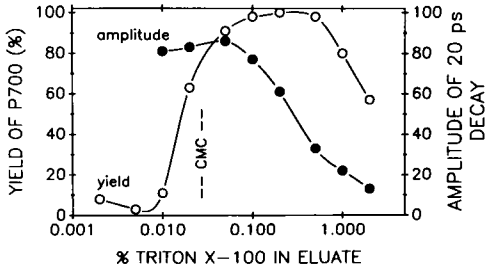

FIGURE 3 Stability and yield of PS I preparations from barley using the modified Triton X-100/hydroxylapatite procedure. Yield of P700 (% of maximum, —O—) and amplitude of the fast decay component (●—) were measured in samples eluted at various Triton X-100 concentrations from a single preparation. *CMC*, critical micelle concentration of Triton X-100 in 0.2 M Na phosphate.

TABLE II
EFFECTS OF ARTIFICIAL ELECTRON DONORS AND ACCEPTORS AND REDOX MEDIATORS ON THE FLUORESCENCE DECAY KINETICS OF A PS I REACTION CENTER/CORE ANTENNA PREPARATION

Additions	A_1	τ_1	A_2	τ_2
None	89.1	22.1	10.9	6126
MV, ascorbate	86.9	21.3	13.1	6129
Ferricyanide	87.1	19.5	12.8	6283
Dithionite	86.4	41.8	13.6	6395
Dithionite*	85.7	20.8	14.3	6399

chl *a*/P700 = 24; source, barley seedlings.
*Sample was oxidized by stirring in air for 30 min after measurement in the presence of dithionite sufficient to block P700 photobleaching.

dithionite sufficient to completely block steady-state P700 photooxidation by reduction of PS I acceptors increased the lifetime of the fast decay component by a factor of 2. The effect of dithionite was completely reversible after oxidation of the sample in air.

Spectral Analysis of the Decay Components

The relative fluorescence emission spectra (excitation at 650 nm, chl *a*/P700 = 33) for the fast (20 ps) and slow (6 ns) decay components are shown in Fig. 4. The fast decay component exhibits a broad emission maximum between 680 and 690 nm and a rapid decline in emission at wavelengths >695 nm. The emission spectrum of the fast decay component was nearly identical in all samples independent of excitation wavelengths between 630 and 670 nm. The emission spectrum of the slow decay component also reveals a broad maximum between 680 and 690 nm. Both decay components exhibited significant emission at wavelengths >700 nm; normalizing the spectra of the fast and slow decay components shows that the slow decay component contains a greater proportion of pigments contributing to the long wavelength (>700 nm) emission. Samples containing chl *b* did not show significant alterations in the shape of the emission spectrum of the fast

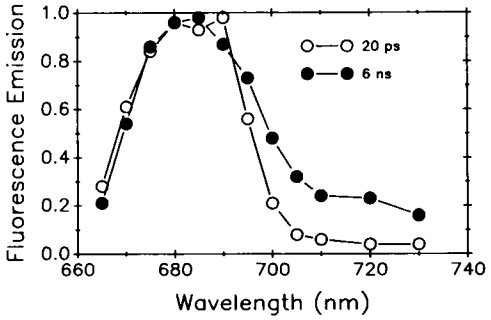

FIGURE 4 Time-resolved fluorescence emission spectra of the fast and slow decay components in a PS I barley preparation (chl *a*/P700 = 33). Spectra were normalized at their relative maxima for comparison (absolute magnitude of the 6 ns decay is ~13% of the normalized spectrum). Excitation at 650 nm.

component but the emission spectrum of the slow decay component showed a increased contribution at wavelengths <680 nm (not shown).

The contribution of the individual decay components to steady-state fluorescence emission can be estimated by integrating the time-resolved decay for each component ($=A_i\tau_i$) and normalizing this product to a constant measuring time and excitation intensity. These calculations (Fig. 5) indicate that steady-state fluorescence emission is almost entirely derived from pigments that contribute to the slow decay component, even though the slow component accounts for only a few percent of the total time-resolved amplitude. Except for a 2-nm blue shift of unknown origin, summing the contributions of both decay components accurately reproduces the measured steady-state emission spectrum.

The relative fluorescence excitation spectra for the fast (20 ps) and slow (6 ns) decay components are shown in Fig. 6. The shape of the two curves is very similar and their sum very closely approximates the steady-state absorption spectrum. The lifetime of the 20 ps decay component varied by $<\pm 6\%$ between 630 and 690 nm excitation, whereas the 6-ns decay generally increased over the entire excitation range. Using the integrated area under the excitation curves as an estimate of absorption cross-section, the data indicate that between 2 and 18% of the pigments present in the preparation contribute to the slow decay component. Samples containing peripheral antenna pigments showed an increase in excitation between 650 and 670 nm for both the fast and slow decay components (not shown).

The excitation and emission wavelength dependence of the fluorescence lifetime in a PS I preparation (chl *a*/P700 = 33) is shown in Fig. 7. The lifetime of the fast-decay component was observed to be relatively constant at emission wavelengths <695 nm (18 ± 2 ps) but increased to 35 ps at 730 nm (Fig. 7 *A*). This pattern was very similar for excitation at 630, 650, and 670 nm. In contrast, the lifetime of the slow decay component decreases with increasing emission wavelength (Fig. 7 *B*). In addition, the lifetime of the slow decay component at a fixed emission

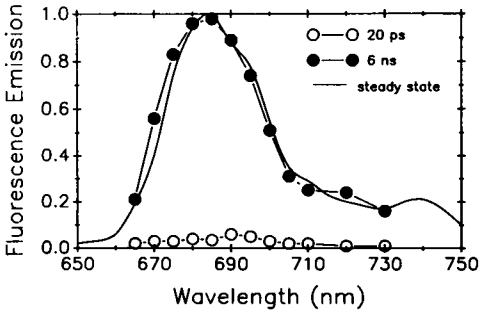

FIGURE 5 Calculated contributions of the fast (—O—) and slow (—●—) decay components of a PS I preparation to steady-state fluorescence emission. Fast decay is shown relative to the slow decay. (*Solid line*) Measured steady-state fluorescence emission spectrum. Calculated from data presented in Fig. 4.

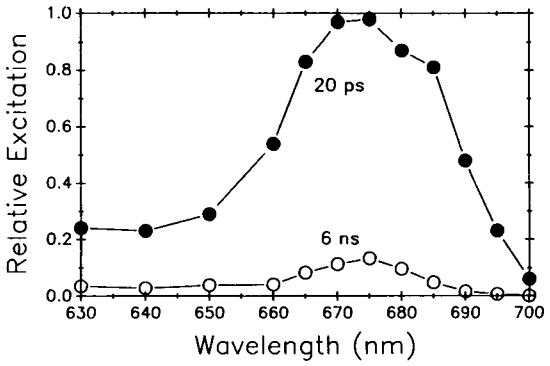

FIGURE 6 Time-resolved fluorescence excitation spectra for the fast and slow decay components in a PS I preparation from barley (chl *a*/P700 = 33). The amplitude of the 6-ns decay (—O—) is shown relative to that of the 20 ps (—●—) component. Emission measured at 715 nm.

wavelength increases with increasing excitation wavelength. Experiments have shown that variations in lifetime of this magnitude cannot be attributed to wavelength-dependent properties of the monochromator–microchannel plate detector combination (Webb, S. P. and T. G. Owens, unpublished results). In comparing different preparations at any given emission wavelength, the lifetime of the fast component generally increased with increasing core antenna size. It was previously demonstrated that the lifetime of the fast decay component in PS I preparations is linearly related to the core antenna size of the preparation (8). However, the relationship between antenna size and lifetime does not extend to samples containing peripheral antenna pigments. In these samples, the lifetime of the fast component remained at 35–40 ps independent of the

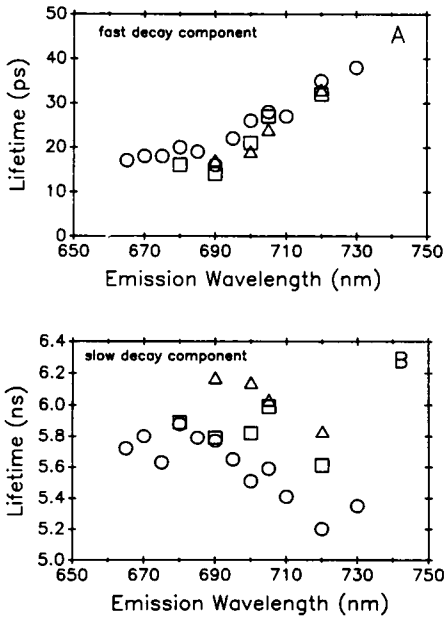

FIGURE 7 Emission wavelength dependence of the fluorescence lifetimes of the fast (*A*) and slow (*B*) decay components in PS I preparations from barley (chl *a*/P700 = 33, 43). (*Circles*) 630 nm excitation. (*Squares*) 650 nm excitation. (*Triangles*) 670 nm excitation.

chl/P700 ratio and of excitation wavelength (650–680 nm). A similar situation was observed in mutants of *C. reinhardii* lacking the PS II reaction center/core antenna complexes (8, 26).

We have also examined the effect of temperature in the range of −20 to 20°C on fluorescence lifetimes in isolated PS I preparations from barley (chl *a*/P700 = 24, samples diluted 1:1 with glycerol, Fig. 8). Samples were counted for <5 min at temperatures >10°C (≈5,000 counts in peak channel) to minimize amplitude losses of the fast decay component induced by increased temperature. Linear regression of the data shows that the lifetime of the fast decay component increased by 9% over the temperature range (14.3 ps at −20°C, 15.2 ps at 20°C). Experimental errors are such that the slope of the regression is not significantly different from zero at $P = 0.95$. The observed relationship between core antenna size and lifetime of the fast decay component for samples as small as 24 chl *a*/P700 (8) suggests that the 15-ps lifetime is above the minimum resolution of our system.

Several treatments were observed to alter the amplitudes of the fast and slow decay components without significantly affecting their lifetimes. These included mild heat treatment (5 min at 30°C), addition of Triton X-100 to a final concentration of >0.2% and aging of the preparation for >24 h at 5°C in the dark. These treatments also caused a blue-shift in the absorption maximum of the preparation to 672 nm, resembling the photochemically active SDS/Triton X-100 PS I preparation of Vierling and Alberte (37). Chlorophyll concentrations in the samples did not change significantly but the amount of P700 decreased by 10–40%.

DISCUSSION

Temporal and Spectral Properties of the Fluorescence Decay

Enriched PS I preparations isolated from barley and *C. reinhardii* that lack chl *b* and the peripheral light-harvesting antenna, and complexes from *Synechococcus* that have low chl/P700 ratios (<45) exhibit well-defined biphasic decay kinetics with lifetimes of 20–40 ps and 6 ns (Table I). The steady-state (14–17) and time-resolved (34, 35) properties of these preparations are similar to other PS I reaction center/core antenna isolates. The major differences produced by the modified Triton X-100/hydroxylapatite procedure used in this investigation are the increased stability of the fast-decay component, reduction in the amplitude of the slow, 6-ns component, and the reduced composition of polypeptides in the 10–20 kD range (subunits II–VI) (20). Our preparations probably retain PS I acceptors A_0, A_1, and F_x, which are associated with the 60–70 kD polypeptides of PS I (19). The modified isolation procedure used in this investigation accommodates monitoring of the chl/P700 ratio and the chl *b* content during the isolation and produces a maximum yield of stable PS I reaction center/core antenna complexes.

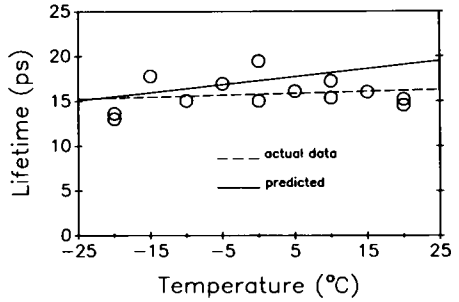

FIGURE 8 Effect of temperature on the fluorescence lifetime of the fast decay component in a PS I preparation from barley (chl *a*/p700 = 24). (*Circles*) Fluorescence lifetime measurements. (*Dashed line*) Linear regression of lifetime data against temperature ($r^2 = 0.92$). (*Solid line*) Dependence of lifetime on temperature predicted from theoretical description of excitation migration in PS I (see text for details).

In a previous investigation, the fast 15–30–ps decay component in enriched PS I preparations was attributed to excitations whose lifetime was limited by efficient photochemical quenching on P700 (8, 26). The decay of excitations in PS I in chloroplasts and intact algae has been assigned to a 40–90–ps time constant (5). The shorter lifetimes in our samples reflect the smaller antenna size (8) resulting from the detergent isolation procedure. The fluorescence excitation spectrum of the fast decay component showed a major contribution from pigments absorbing at 670–680 nm. The corresponding emission spectrum exhibited a broad maximum at 680–690 nm. These spectral properties are characteristic of PS I core pigments (14, 15) indicating that the fast-decay component represents the lifetime of excitations in the PS I core antenna. Assuming a Stokes shift of ~ -130 cm^{-1} (= 6 nm) (36), the similarities of the excitation and emission spectra suggest that the same spectral forms of chl *a* in the core antenna are contributing to both the absorption and fluorescence associated with the fast-decay component.

The lifetime of the slow decay component (5–6 ns) is similar to that of free chl *a* in dilute solution (38) but available evidence does not support the presence of detergent-solubilized chl *a* in our samples. The emission spectrum of the slow component is red-shifted and broadened compared with that of chl *a* in detergent micelles, showing a broad maximum at 680–690 nm similar to the fast component. We were unable to reduce the amplitude of the slow component by further hydroxylapatite chromatography. Several treatments including mild heat or low concentrations (0.2–1%) Triton X-100 or lithium dodecyl sulfate (LDS), were observed to increase the amplitude of the slow component at the expense of the fast component but without altering the lifetime of either component. These treatments resulted in an irreversible inhibition of P700 photooxidation without significantly decreasing the chlorophyll content of the samples. LDS treatment was specifi-

cally shown to inhibit PS I photochemistry without causing dissociation of pigments from the reaction center/core antenna complex (8). We therefore attribute the slow decay component to PS I core antenna pigments that are unable to transfer excitation energy to P700.

Time-resolved excitation spectra indicate that the slow-decay component accounts for 2–18% of the absorption cross-section of our enriched preparations. One interpretation of these data is that each reaction center/core antenna complex contains a small fraction of core antenna pigments which do not function in energy transfer to the reaction center. Alternatively, 2–18% of the complexes may not contain a functional reaction center. These explanations are not mutually exclusive and it is difficult to assess the degree of heterogeneity in these samples. We support the hypothesis of core antenna complexes without functional traps because of the similarity in the time-resolved excitation and emission spectra of the two decay components, and because the lifetime of the fast-decay component does not change in response to treatments that increased the amplitude of the flow decay component to 80% of the total decay. Such a decrease in lifetime would be expected as the result of the smaller effective antenna size of functional reaction center/core antenna aggregates (8). There is no evidence for a 5–6–ns decay component in intact algal cells or chloroplasts or in *C. reinhardii* mutants missing the PS II reaction center (8, 11, 33).

The lifetimes of the fast- and slow-decay components in PS I show an unusual emission wavelength-dependence. The fast component exhibited a lifetime that was essentially constant at wavelengths <695 nm but increased with increasing wavelength >700 nm. This pattern was independent of excitation wavelength between 630 and 670 nm. A similar dependence was observed in whole cells of *Chlorella* for a PS I decay component (lifetime = 30–60 ps) (12). The slow component of our preparations generally decreases in lifetime with increasing emission wavelength. A different wavelength dependence for the three major decay was observed in whole cells of *Chlorella* (10) and *C. reinhardii* (40), but in these studies the fast-decay component (150 ps) contained contributions from both PS I and PS II.

The core antenna of PS I probably consists of several spectral forms of chl *a*. Due to limitations in the information content of photon counting decay curves with a finite number of data points, a least-squares fit is unable to resolve decay components with similar lifetimes (e.g., 20 and 40 ps). If the pigment pools that contribute to a temporally unresolved decay have distinct spectral properties, the unresolved decay may display a lifetime that varies with excitation or emission wavelength. Alternatively, the wavelength dependence of the fast decay may be related to the dynamics of excited state processes in the core antenna. For the fast component, the break in the distribution of lifetimes coincides with the absorbance of P700. Increasing lifetimes at wavelengths >700 nm may reflect thermally activated energy transfer to the trap from pigments whose relaxed excited state energy lies below P700. In either case, the wavelength-dependent lifetimes in PS I reported here have important implications for global analysis techniques (33) that assume that the lifetime of a decay component is independent of emission wavelength. The global procedure also implicitly assumes that each decay component is derived from a homogeneous population of pigment molecules.

Intermediate Lifetime Components

The presence of chl *b* and peripheral antenna complexes in our PS I preparations resulted in the loss of biphasic kinetics in the fluorescence decay. Time-resolved fluorescence analyses have previously revealed multiexponential decays in isolated PS I reaction center preparations (34) and in mutants of *C. reinhardii* that lack the PS II reaction center/core antenna complex (11, 26). The association of chl *b* with PS I was demonstrated by the comigration of chl *b* and P700 during centrifugation of continuous sucrose gradients, and by the contribution of chl *b* at 652 nm to the excitation spectrum of the fast decay component. Lifetimes in the 1.5–2.5–ns range are characteristic of some isolated peripheral light-harvesting complexes (11, 40, 41). The presence of uncoupled peripheral antenna complexes can be easily distinguished by their time-resolved excitation and emission spectra (26).

Lifetimes in the 150 to 450–ps range in PS I have been noted by several investigators (34, 35) but have not been explained satisfactorily. Charge recombination reactions between $P700^+$ and reduced acceptors A_0, A_1, and F_x (A_2) occur on time scales slower than 5 ns (19, 42). In time-resolved absorption studies of PS I preparations with chl *a*/P700 ratios >50 (chl *b* content not reported), there is no evidence for photochemical reactions contributing in the 150–450–ps time range (43–46). However, the limited dynamic range of pump-probe absorption measurements may preclude detection of low-amplitude components. The time-resolved excitation and emission spectra of a 250 ps component have been measured in mutants of *C. reinhardii* missing the PS II reaction center/core antenna complex (26). These data show an emission spectrum clearly characteristic of the core antenna pigments and an excitation spectrum with contributions from both the peripheral and core antenna pigments. The in vitro measurements of this study are very similar, differing only in minor spectral shifts due presumably to the action of Triton X-100 in the isolation procedure. These spectral features and the absence of intermediate lifetime components in reaction center/core antenna preparations lacking chl *b*, suggest the 150–450–ps components originate as the result of interactions between the peripheral and core antenna pigments which induce the formation of minor pigment aggregates in the core antenna. The ability of these aggregates to transfer excitation energy to P700 has not been established.

The contribution of chls *a* and *b* in the peripheral antenna (650–670 nm) to the excitation spectrum of the fast-decay component in samples containing chl *b* indicates that excitation transfer from the peripheral to the core antenna aggregates must be rapid compared with the lifetime of excitations in the core antenna. In *C. reinhardii* mutants missing the PS II reaction center, the overall decay kinetics and core antenna lifetime are independent of excitation wavelength even when 95% of the excitations originate on chl *b* (26). Peripheral to core antenna transfer times were estimated to be <5 ps (26). In the present study, excitation at 652 nm in samples containing chl *b* did not alter the kinetics of the fluorescence decay compared with 680 nm excitation, even though the excitation spectrum clearly shows energy transfer from chl *b* to the core antenna pigments. In both cases, emission from chl *a* or chl *b* in the peripheral antenna was not observed in the emission spectrum of the fast-decay component. In addition, we did not observe rise components of any lifetime in the time-resolved fluorescence properties of the core antenna pigments, even though a rise was frequently included in the initial estimates for the fitting routines. Thus, it is unlikely that the 150–350 ps intermediate decay component is associated with excitation transfer between the peripheral and core antenna complexes.

PS I Variable Fluorescence

It is generally accepted that PS I exhibits little or no variable fluorescence in vivo or in enriched PS I preparations (47). Our data indicate that in PS I reaction centers in the open state (P700 A_0) and in states $P700^+$ A_0 and P700 $(A_0 A_1 F_x)^-$ are both efficient at quenching excitation in the PS I core antenna. This is general agreement with the data of Kamagowa et al. (35) in work with highly enriched PS I samples (8–10 chl *a*/P700). Our data shows that reduction of the primary acceptor of PS I increased the lifetime by only a factor of 2. In contrast, irreversible inhibition of P700 photochemistry by mild LDS treatment increased the lifetime × 300 (8). Thus the short lifetime of excitation in the core antenna of PS I depends on the presence of a functional trap but not on the redox state of the primary donor or acceptors. Because of the low probability of detrapping in PS I (8), these data also would preclude cooperativity between PS I units in either the open or closed states.

A second factor complicates the interpretation of fluorescence yield from enriched PS I preparations. Calculation of the steady-state fluorescence yield by integration of the two decay components indicates that the slow component contributes >95% of the steady-state fluorescence even though it may account for <5% of the time-resolved decay. As a result, steady-state fluorescence should be insensitive to the redox state of the trap or to the presence of a functional trap. We were unable to detect steady-state changes in fluorescence yield after oxidation of reduction of our preparations. In a highly enriched preparation (8–10 chl *a*/P700), Ikegami (17) observed a moderate fluorescence increase with reduction of the PS I acceptors. It is possible that their nonaqueous isolation procedure yield samples that lack a slow decay component.

Spectral Composition and Structure of the Core Antenna

In agreement with previous investigations (15), the spectral characteristics of our PS I preparations indicate that the PS I core antenna is composed of several spectral forms of chl *a*. Although samples are heterogeneous in terms of fluorescence lifetimes, the absorption and fluorescence spectra of the core antenna appear to be insensitive to the presence or absence of P700. In addition, these properties are independent of the core antenna size of the preparation. Because the time-resolved fluorescence excitation and emission spectra of the dominant decay components (20 ps, 6 ns) in the enriched preparations are so similar, spectral analyses based upon the steady-state spectra is justified. We have analyzed the spectral properties of our samples using gaussian deconvolution of the spectra. Deconvolution of either the absorption (600–750 nm) or the fluorescence emission (600–800 nm) requires a minimum of four components to fit the spectra with errors <2.5% (Table III).

TABLE III
GAUSSIAN DECONVOLUTION OF THE STEADY-STATE ABSORPTION (600–750 nm) AND FLUORESCENCE EMISSION (600–800 nm) SPECTRA OF A PS I PREPARATION

Absorption Spectra					
Four Components			Five Components		
Maximum	Bandwidth	Amplitude	Maximum	Bandwidth	Amplitude
Q_x transition					
614	37.8	0.167	612	51.2	0.146
639	36.9	0.179	640	41.4	0.166
Q_y transition					
674	28.5	0.707	667	21.6	0.381
681	22.8	0.321	677	20.0	0.507
			685	21.9	0.387
Error = 2.01%			Error = 1.81%		
Fluorescence emission spectra					
Four components			Five components		
Maximum	Bandwidth	Amplitude	Maximum	Bandwidth	Amplitude
Primary maximum					
678	20.2	0.680	678	19.6	0.667
691	22.4	0.666	682	28.5	0.121
			693	20.6	0.601
Secondary maximum					
715	22.0	0.181	712	13.8	0.151
738	25.3	0.191	733	30.3	0.225
Error = 2.37%			Error = 2.16%		

chl *a*/P700 = 43; source, barley seedlings.

Although increasing the number of gaussians resulted in smaller errors, modeling spectral with a minimum number of components permits an evaluation of excitation transfer in the core antenna.

The absorption spectrum is equally well described by the sum of four or five gaussians (2 in the Q_x envelope and 2 or 3 in the Q_y). The four-component analysis yields two gaussians in the Q_y region with maxima at 674 and 681 nm but with different bandwidths. Addition of a third component in the Q_y absorption produces a new component at 667 nm, small red shift of the other maxima and equal bandwidth for all Q_y components. Deconvolution of the fluorescence emission spectrum also requires a minimum of four components to accurately fit the data, two components in the primary emission maximum (678 and 691 nm) and two in the secondary maximum. In contrast to the absorption data, addition of a third component in the primary maximum does not lead to the appearance of a new spectral form fluorescing in the short-wavelength region. Assuming a Stokes shift of 6 nm (36), a spectral form absorbing at 667 nm should fluoresce near 673 nm. The deconvolution data do not support a distinct emission component at this wavelength.

Although the lifetimes of the various spectral forms of chl *a* in the PS I core antenna pigments are not resolved in our analyses, the spectral forms can be distinguished by their relative contributions to the time-resolved excitation and emission spectra. This permits a description of excitation migration within the core antenna. The gaussian deconvolution data indicate the three major core antenna components absorb at 667, 677, and 685 nm with relative amplitudes of 0.8:1.0:0.8. The fluorescence emission maxima are at 678 and 691 nm with nearly equal amplitudes. The gaussian analysis does not indicate a distinct emission component associated with the 677 nm absorption but the time-resolved emission spectra of the 20 ps and 6 ns decays both show emission at 673 nm that is ~60% of the maximum amplitude. These emission data indicate that over the lifetime of excitations in the core antenna, excitation energy is not entirely concentrated in the longest wavelength absorbing forms but is nearly homogenized among all spectral forms present. Comparison of the relative absorption and emission amplitudes shows a slight (≈20%) concentration of excitations in progressively longer wavelength pigments. A rapid homogenization of excitations among the core antenna spectral forms is also supported by the constant core antenna lifetime observed for excitation between 650 and 690 nm.

In computer simulations that assume positions and orientations of the pigments within a model PS I core antenna array, Gulotty (48) demonstrated that a concentric organization of two spectral forms (675 and 685 nm) around a reaction center (P700) with the longer wavelength form closest to the trap, leads to a rapid (<5 ps) concentration of excitations in the long-wavelength pigments. When the spectral forms were randomly distributed around the reaction center, the excitation was homogenized between the two spectral forms on a subpicosecond time scale. These simulations do not take into account the possible contributions of nonrandom position and orientation of core antenna pigments but do provide examples of two limiting cases of excitation dynamics in antenna aggregates containing multiple spectral forms.

The similarity of the absorption spectra in preparations with different core antenna sizes indicates that the relative distribution of core antenna spectral forms is not altered by procedures that reduce the size of the core antenna. A similar ratio of short (<680 nm) to long (>680 nm) wavelength absorbing pigments has been reported in highly enriched PS I preparations (chl *a*/P700 = 8–10) (17) and in *C. reinhardii* mutants lacking PS II (26). There are two possible explanations for the insensitivity of the absorption properties to changes in PS I core antenna size. First, the consistency of the ratio may be due to the coordinated loss of pigment binding sites in clusters of pigments through partial denaturation or complete loss of pigment binding subunits. Shubin et al. (49) have reported that the PS I reaction center/core antenna complex contains five to seven identical clusters of pigments (six to eight chl *a*) and an additional cluster that also contains P700. Alternatively, the two pigment forms may not be located concentrically around the trap with the longer wavelength forms closer to the trap as proposed by the "funnel" models of antenna structure and excitation energy transfer (50). Rather the spectral forms may be arranged in a more random fashion such that sequential removal of the outer pigments by detergent action may not alter the relative abundances of spectral forms remaining. The former would lead to a discontinuous distribution of chl *a*/P700 ratios with antenna sizes differing by as much as 15–30 chls per P700, whereas the latter would lead to a more continuous distribution. Because the lifetime of the fast component was shown to vary with core antenna size (~0.5 ps/chl) (8), the discontinuous distribution would result in multiple fast-decay components. Unfortunately, analysis of simulated decays with gaussian noise indicate that our data regression routines may not distinguish between the decay of a sample with a uniform 45 chl/P700 and one with a bimodal distribution of 30 and 60 chls/P700. We routinely checked our data for the presence of multiple decay components in the 15–50–ps range but find no evidence to support their existence.

Analysis of the contribution of core antenna spectral forms to the time-resolved excitation and emission spectra, the model core antenna calculations and the lack of variation in the spectral properties with core antenna size all suggest that the rapid homogenization of excitations among the core antenna spectral forms may be related to a more random distribution of spectral forms around the trap than that predicted by the funnel model. Similarly, one would not predict the observed linear relationship between PS I core antenna size and fluorescence lifetime

(8) if excitations were concentrated in the long wavelength forms of the antenna. These data suggest that the funnel model of antenna structure, with the longer wavelength absorbing antenna forms nearest the trap, should be reexamined with respect to PS I. Our data also indicate that the removal of the trap does not alter the pattern of excitation dynamics in the core antenna.

Excitation Transfer in the Core Antenna

Based upon the observed linear dependence of excitation lifetime on PS I core antenna size, we have used equations from the theoretical treatment of Pearlstein (51) to evaluate the dynamics of excitation migration and photochemical trapping in PS I (8). Although Pearlstein's treatment involved regular two- and three-dimensional lattice arrays containing a reaction center and a single spectral form of antenna pigment, our data support the application of these equations to excitation dynamics in PS I and predict a time constant for photochemical charge separation of 3.1 ± 0.7 ps (8). The average single-step transfer time for excitation transfer between adjacent antenna sites was 0.21 ps which corresponds to a rate constant for Förster energy transfer of $\approx 1 \times 10^{12}\ s^{-1}$. This relatively large rate constant may have important implications for the core antenna structure and mechanism of energy transfer.

Assuming maximum values for the relative orientation factor of the donor and acceptor transition dipoles ($K^2 = 4$) and the Förster overlap integral ($I = 0.53$) (36), a Förster rate constant of $1 \times 10^{12}\ s^{-1}$ predicts an upper limit of 16.8 A for the intermolecular spacing (center to center) of coupled pigments in the core antenna. Suboptimal values of K^2 and I would necessarily lead to smaller separations. This value is below the limit of 25 A for calculation of Förster overlap integrals (36). At separations <25 A, excitonic (coherent) effects may begin to contribute to excitation migration as the dipole–dipole interaction energy between donor and acceptor approaches the energy of intramolecular vibrational transitions (2). These effects may be responsible for the multiple CD signals associated with PS I preparations (49) although these signals probably arise from pigments restricted to the immediate vicinity of P700 (52). Because theoretical considerations indicate that coherent effects are lost for excitation lifetimes >1 ps (2), the errors resulting from use of equations derived in the Förster limit are probably small.

The linear dependence of fluorescence lifetime on PS I core antenna size also predicts that excitation migration in PS I is nearly diffusion limited, with each excitation making an average of 2.4 visits to the reaction center before being quenched by photochemistry (8). The average trapping time in the array (0.21 ± 0.05 ps) is comparable with the average time for transfer between antenna pigments (0.21 ± 0.04 ps), whereas the average detrapping time is much longer (2.4 ± 0.5 ps). Thus the dynamics of excitation transfer reactions between the core antenna and P700 are largely determined by the rates of photochemistry and detrapping. The comparable rates of trapping and antenna transfer explain the similar emission properties of the core antenna in the presence and absence of P700.

In the diffusion limit of excitation migration, the effect of temperature on the lifetime of an excitation is expected to be small because the principle temperature-dependent process is the rate of detrapping. This was confirmed by measuring the lifetime of PS I core antenna excitations between −20° and 20°C (Fig. 8). Using the Boltzmann distribution to evaluate the temperature dependence of the detrapping rate in an array with 24 antenna sites per reaction center, calculations (based on Eq. 3, reference 8) predict an increase in lifetime of 23% (15.5–19.0 ps) over the same temperature range. The actual data (Fig. 8) show a somewhat smaller increase of 9%, indicating that the model calculations may underestimate the extent of detrapping in PS I. This difference is most likely accounted for by our assumption that the Stokes shift of the reaction center pigments is the same as that of the core antenna pigments (8). These data indicate that excitation migration in the core antenna of PS I approaches the diffusion limit, with an excitation making two to four visits to P700 before being utilized in photochemical charge separation.

The description of excitation migration in PS I as approaching diffusion limitation, and at the same time having the excited state nearly homogenized among the core antenna spectral forms during the lifetime of the excitation, does not necessarily create a contradiction. As stated above, diffusion versus trapping limited excitation migration is largely controlled by the relative rate constants for photochemistry, trapping, and detrapping. Homogenization of the excitation among the core antenna spectral forms results from an excitation, on the average, visiting a representative distribution of all spectral forms during its lifetime. Because the temporal and spectral properties of the fluorescence decay represent the weighted average of all possible excitation migration pathways, the decay will be a complex function of antenna structure. However, the extent of homogenization will be largely determined by the spatial location of each spectral form within the complex (48) and the rate constants for energy transfer between all core pigments (including P700).

SUMMARY AND CONCLUSIONS

(*a*) Photosystem I reaction center/core antenna preparations that lack chl *b* have fluorescence decays accurately described by two widely separated exponentials. The excitation and emission spectra of both components are very similar. The dominant fast decay (20–40 ps) results from photochemical quenching on P700. We suggest that the slow decay (6 ns) originates from core antenna aggregates lacking a functional trap. Steady-state fluorescence emission is dominated (>90%) by the slow decay.

(*b*) The lifetime of the fast decay is constant at emission wavelengths <700 nm but increases at greater wavelength. This may reflect thermally activated transfer to the trap

from core pigments whose relaxed excited state energy is lower than P700.

(c) Intermediate lifetime decays (150–350 ps) are observed in preparations containing chl *b* and peripheral antenna complexes. The fast-decay component retains the same lifetime it has in chl *b*–less samples regardless of excitation wavelength. No rise components in the core antenna emission are detected, even when the majority of the excitations originate in the peripheral antenna. The lack of peripheral antenna emission in the fluorescence spectrum of the fast decay suggests that transfer from peripheral to core antenna is very rapid.

(*d*) Reduction of the acceptors of PS I increases the lifetime of the fast decay by a factor of two. The effect is completely reversible. In PS I reaction centers in the open state (P700 A_0) or in state $P700^+$ A_0 are equally efficient quenchers. Combined with the low probability of detrapping in PS I, these factors limit cooperativity between PS I units in either open or closed states.

(*e*) The PS I core antenna contains several spectral forms of chl *a*. The time-resolved excitation and emission spectra of the core antenna do not depend on the presence of P700 and do not vary as a function of core antenna size. The time-resolved spectra show that excitations are not concentrated in the longest wavelength absorbing forms but are nearly homogenized among all spectral forms during the lifetime of the excitation. These data suggest that the "funnel" model for antenna organization does not apply to the PS I core antenna.

(*f*) Excitation migration in PS I is nearly diffusion limited. The predicted effect of temperature on the rate of detrapping and fluorescence lifetime was confirmed by measurements in the −20-to-20° range.

We wish to thank D. Eads and E. Castner for technical assistance with the laser systems, E. Wold for assistance with the PS I preparations, and R. Gulotty for his initial work on the model system calculations.

This research was supported by grants from the National Science Foundation (DMB 8509590 and DCM 8409014). T.G.O. was supported by a National Institutes of Health postdoctoral fellowship; S.P.W. was supported by a gift from Amico Corporation.

REFERENCES

1. Zuber, H. 1985. Structure and function of light-harvesting complexes and their polypeptides. *Photochem. Photobiol.* 42:821–844.
2. Knox, R. S. 1977. Photosynthetic efficiency and exciton transfer and trapping. *Top. Photosynth.* 2:55–97.
3. Pearlstein, R. M. 1982. Chlorophyll singlet excitons. *In* Photosynthesis. Vol. 1. Energy Transfer in Plants and Bacteria. Govindjee, editor. Academic Press, New York. 293–330.
4. Pertich, J. W., and G. R. Fleming. 1984. Ultrafast processes in biology. *Photochem. Photobiol.* 40:775–780.
5. Geacintov, N. E., and J. Breton. 1987. Energy transfer and fluorescence mechanisms in photosynthetic membranes. *CRC Crit. Rev. Plant Sci.* 5:1–44.
6. Cross, A. J., and G. R. Fleming. 1984. Analysis of time-resolved fluorescence anistropy decays. *Biophys. J.* 46:45–56.
7. Holzwarth, A. R., J. Wendler, and G. W. Suter. 1987. Studies on chromophore coupling in isolated phycobiliproteins II. Picosecond energy transfer kinetics and time-resolved fluorescence spectra of C-phycocyanin from *Synechococcus* 6301 as a function of aggregation state. *Biophys. J.* 51:1–12.
8. Owens, T. G., S. P. Webb, L. Mets, R. S. Alberte, and G. R. Fleming. 1987. Antenna size dependence of fluorescence decay in the core antenna of photosystem I: estimates of charge separation and energy transfer rates. *Proc. Natl. Acad. Sci. USA.* 84:1532–1536.
9. Sheer, H. 1987. Energy transfer and photochemistry of C-phycocyanin. *In* Progress in Photosynthesis Research. Vol. 1. J. Biggins, editor. Martinus Nijhoff, The Hague.
10. Holzwarth, A. R., J. Wendler, and W. Haehnal. 1985. Time-resolved picosecond fluorescence of the antenna chlorophylls in *Chlorella vulgaris*. Resolution of photosystem I fluorescence. *Biochim. Biophys. Acta.* 807:155–167.
11. Gulotty, R. J., L. Mets, R. S. Alberte, and G. R. Fleming. 1985. Picosecond fluorescence study of photosynthetic mutants of *Chlamydomonas reinhardii:* origin of the fluorescence decay of chloroplasts. *Photochem. Photobiol.* 41:487–496.
12. Hodges, M., and I. Moya. 1986. Time-resolved chlorophyll fluorescence studies of photosynthetic membranes: resolution and characterization of four kinetic components. *Biochim. Biophys. Acta.* 849:193–202.
13. Kyle, D. J., N. Baker, and C. J. Arntzen. 1983. Spectral characterization of photosystem I fluorescence at room temperature using thylakoid protein phosphorylation. *Photobiochem. Photobiophys.* 5:11–25.
14. Mullet, J. E., J. J. Burke, and C. J. Arntzen. 1980. Chlorophyll proteins of photosystem I. *Plant Physiol. (Bethesda).* 65:814–822.
15. Shiozawa, J. A., R. S. Alberte, and J. P. Thornber. 1974. The P700-chl a-protein. Isolation and some characteristics of the complex in higher plants. *Arch. Biochem. Biophys.* 165:388–397.
16. Bengis, C., and N. Nelson. 1975. Purification and properties of the photosystem I reaction center from chloroplasts. *J. Biol. Chem.* 250:2783–2788.
17. Ikegami, I. 1976. Fluorescence changes related to the primary photochemical reaction in the P700-enriched particles isolated from spinach chloroplasts. *Biochim. Biophys. Acta.* 449:245–258.
18. Takahashi, Y., K. Hirota, and S. Katoh. 1985. Multiple forms of P700-chlorophyll a-protein complexes from *Synechococcus sp.:* the iron, quinone and carotenoid contents. *Photosynth. Res.* 6:183–192.
19. Golbeck, J. H., and J. M. Cornelius. 1986. Photosystem I charge separation in the absence of centers A and B. I. Optical characterization of center "A_2" and evidence for its association with a 64-kDa peptide. *Biochim. Biophys. Acta.* 849:16–24.
20. Bengis, C., and N. Nelson. 1977. Subunit structure of the photosystem I reaction center. *J. Biol. Chem.* 252:4564–4569.
21. Okamura, M. Y., G. Feher, and N. Nelson. 1982. Reaction centers. *In* Photosynthesis. Vol 1. Energy Conversion by Plants and Bacteria. Govindjee, editor. Academic Press, New York. 195–274.
22. Wollman, F.-A., and P. Bennoun. 1982. A new chlorophyll-protein complex related to photosystem I in *Chlamydomonas reinhardii. Biochim. Biophys. Acta.* 680:352–360.
23. Haworth, P., J. L. Watson, and C. J. Arntzen. 1983. The detection, isolation and characterization of a light-harvesting complex which is specifically associated with photosystem I. *Biochim. Biophys. Acta.* 724:151–158.
24. Anderson, J. M., J. S. Brown, E. Lam, and R. Malkin. 1983. Chlorophyll b: an integral component of photosystem I of higher plant chloroplasts. *Photochem. Photobiol.* 38:205–210.
25. Ish-Shalom, D., and I. Ohad. 1983. Organization of chlorophyll-protein complexes of photosystem I in *Chlamydomonad reinhardii. Biochim. Biophys. Acta.* 722:498–507.

26. Owens, T. G., S. P. Webb, D. D. Eads, R. S. Alberte, L. Mets, and G. R. Fleming. 1987. Time-resolved fluorescence decay in photosystem I: experimental estimates of charge separation and energy transfer rates. *In* Progress in Photosynthesis Research. Vol 1. J. Biggins, editor. Martinus Nijhoff, The Hague. 83–86.
27. Surzycki, S. 1971. Synchronously grown cultures of *Chlamydomonas reinhardii*. *Methods Enzymol.* 23:67–73.
28. Guillard, R. R. L., and J. H. Ryther. 1962. Studies on marine plankton diatoms. *Cyclotella nana* (Huestedt) and *Detonula confervaceae* (Cleve). *Can. J. Microbiol.* 8:229–239.
29. Jeffery, S. W., and G. F. Humphrey. 1975. New spectrophotometric equations for determining chlorophylls a, b, c_1 and c_2 in higher plants, algae and natural phytoplankton. *Biochem. Physiol. Pflanz. (BPP).* 167:191–194.
30. Hayama, T., and B. Ke. 1972. Difference spectra and extinction coefficients of P700. *Biochim. Biophys. Acta.* 267:160–171.
31. Thornber, J. P. 1969. Comparison of the chlorophyll-protein complex isolated from a blue-green alga with chlorophyll-protein complexes obtained from green bacteria and higher plants. *Biochim. Biophys. Acta.* 172:230–241.
32. Chang, M. C., S. H. Courtney, A. J. Cross, R. J. Gulotty, J. W. Petrich, and G. R. Fleming. 1985. Time-correlated single photon counting with microchannel plate detectors. *Anal. Instrum.* 14:433–464.
33. Holzwarth, A. R. 1987. A model for functional antenna organization and energy distribution in the photosynthetic apparatus of green plants and green algae. *In* Progress in Photosynthetic Research. Vol 1. J. Biggins, editor. Martinus Nijhoff, The Hague.
34. Holzwarth, A. R., W. Haehnal, J. Wendler, G. Suter, and R. Ratajczak. 1984. Picosecond fluorescence kinetics and energy transfer in antennae chlorophylls of green algae and membrane fractions of thylakoids. *In* Advances in Photosynthesis Research. Vol 1. C. Sybesma, editor. Martinus Nijhoff, The Hague. 73–77.
35. Kamagowa, K., J. M. Morris, Y. Takagi, N. Nakashima, K. Yoshihara, and I. Ikegami. 1983. Picosecond fluorescence studies of P700-enriched particles of spinach chloroplasts. *Photochem. Photobiol.* 37:207–213.
36. Shipman, L. L., and D. L. Housman. 1979. Förster transfer rates for chlorophyll *a*. *Photochem. Photobiol.* 29:1163–1167.
37. Vierling, E., and R. S. Alberte. 1983. P700 chlorophyll a-protein. Purification, characterization and antibody preparation. *Plant Physiol. (Bethesda).* 72:625–633.
38. Brody, S. S., and E. Rabinowitch. 1957. Excitation lifetime of photosynthetic pigments *in vitro* and *in vivo*. *Science (Wash. DC).* 125:555.
39. Haehnal, W., A. R. Holzwarth, and J. Wendler. 1983. Picosecond fluorescence and energy transfer in the antenna chlorophylls of green algae. *Photochem. Photobiol.* 37:435–443.
40. Lotshaw, W. T., R. S. Alberte, and G. R. Fleming. 1982. Low-intensity subnanosecond fluorescence study of the light-harvesting chlorophyll a/b protein. *Biochim. Biophys. Acta.* 682:75–85.
41. Eads, D. D., S. P. Webb, T. G. Owens, L. Mets, R. S. Alberte, and G. R. Fleming. 1987. Characterization of the fluorescence decays of the chlorophyll a/b protein. *In* Progress in Photosynthesis Research. Vol 1. J. Biggins, editor. Martinus Nijhoff, The Hague.
42. Shuvalov, V. A., A. M. Nuijs, H. J. van Gorkum, J. W. J. Smit, and L. M. N. Duysens. 1986. Picosecond absorbance changes upon selective excitation of the primary donor P700 in photosystem I. *Biochim. Biophys. Acta.* 850:319–323.
43. Il'ina, M. D., V. V. Kravsauskas, R. J., Rotomskis, and A.-Y. Borisov. 1984. Difference picosecond spectroscopy of pigment-protein complexes of photosystem I from higher plants. *Biochim. Biophys. Acta.* 767:501–513.
44. Borisov, A.-Y., P. V. Danelius, M. D. Il'ina, V. V. Krasauskas, A. S. Piskarskas, A. P. Razjuim, and R. J. Rotomskis. 1985. Picosecond kinetics and difference absorption changes in pigment-protein complexes of photosystem I. *Mol. Biol. (Mosc.)* 19:636–642.
45. Nuijs, A. M., V. A. Shuvalov, H. J. van Gorkum, J. J. Plijter, and L. N. M. Duysens. 1986. Picosecond absorbance difference spectroscopy of the primary reaction and the antenna-excited states in photosystem I particles. *Biochim. Biophys. Acta.* 850:310–318.
46. Gore, B. L., L. B. Giorgi, and G. Porter. 1987. Picosecond transient absorption spectroscopy of green plant photosystem I reaction centers. *In* Ultrafast Phenomena IV. G. R. Fleming and J. E. Seigman, editors. Springer Verlag, Berlin. 389–401.
47. Butler, W. L. 1978. Energy distribution in the photochemical apparatus of photosynthesis. *Annu. Rev. Plant Physiol.* 29:345–378.
48. Gulotty, R. J. 1985. Excitation transfer and trapping in higher plant photosynthesis. PhD thesis. University of Chicago, Chicago, IL.
49. Shubin, V. V., N. V. Karapetyan, and A. R. Krasnovsky. 1986. Molecular arrangement of pigment-protein complexes of photosystem I. *Photosynth. Res.* 9:3–12.
50. Seely, G. R. 1973. Energy transfer in a model of the photosynthetic unit of green plants. *J. Theor. Biol.* 40:189–199.
51. Pearlstein, R. M. 1982. Exciton migration and trapping in photosynthesis. *Photochem. Photobiol.* 35:835–644.
52. Ikegami, I., and S. Itoh. 1986. Chlorophyll organization in P700-enriched particles isolated from spinach chloroplasts. CD and absorption spectroscopy. *Biochim. Biophys. Acta.* 851:75–85.